

## EVIDENCE FOR A SIGNIFICANT INTERMEDIATE-AGE POPULATION IN THE M31 HALO FROM MAIN SEQUENCE PHOTOMETRY<sup>1</sup>

THOMAS M. BROWN, HENRY C. FERGUSON, ED SMITH

Space Telescope Science Institute, 3700 San Martin Drive, Baltimore, MD 21218; tbrown@stsci.edu, ferguson@stsci.edu, edsmith@stsci.edu

RANDY A. KIMBLE, ALLEN V. SWEIGART

Code 681, NASA Goddard Space Flight Center, Greenbelt, MD 20771; randy.a.kimble@nasa.gov, allen.v.sweigart@nasa.gov

ALVIO RENZINI

European Southern Observatory, Karl-Schwarzschild-Strasse 2, Garching bei München, Germany; arenzini@eso.org

R. MICHAEL RICH

Division of Astronomy, Dpt. of Physics & Astronomy, UCLA, Los Angeles, CA 90095; rmr@astro.ucla.edu

DON A. VANDENBERG

Department of Physics and Astronomy, University of Victoria, P.O. Box 3055, Victoria, BC, V8W 3P6, Canada; davb@uvvm.uvic.ca

*To appear in The Astrophysical Journal Letters*

### ABSTRACT

We present a color-magnitude diagram (CMD) for a minor-axis field in the halo of the Andromeda galaxy (M31), 51 arcmin (11 kpc) from the nucleus. These observations, taken with the Advanced Camera for Surveys (ACS) on the Hubble Space Telescope, are the deepest optical images yet obtained, attaining 50% completeness at  $m_V = 30.7$  mag. The CMD, constructed from  $\sim 3 \times 10^5$  stars, reaches more than 1.5 mag fainter than the old main-sequence turnoff. Our analysis is based on direct comparisons to ACS observations of four globular clusters through the same filters, as well as  $\chi^2$  fitting to a finely-spaced grid of calibrated stellar-population models. We find that the M31 halo contains a major ( $\sim 30\%$  by mass) intermediate-age (6–8 Gyr) metal-rich ( $[\text{Fe}/\text{H}] > -0.5$ ) population, as well as a significant globular-cluster age (11–13.5 Gyr) metal-poor population. These findings support the idea that galaxy mergers played an important role in the formation of the M31 halo.

*Subject headings:* galaxies: evolution – galaxies: stellar content – galaxies: halos – galaxies: individual (M31)

### 1. INTRODUCTION

A primary quest of observational astronomy is to establish the formation history of galaxies. Studies of the stellar populations at the main-sequence turnoff (MSTO) provide the most precise measurements, but these generally have been limited to the Galaxy and its satellites. The Galaxy has driven much of our thinking regarding the formation of giant spirals, with its predominately old metal-poor halo (e.g., Vandenberg 2000; Ryan & Norris 1991) and younger disk (e.g., Sourbiran, Bienaymé, & Siebert 2003; Fontaine, Brassard, & Bergeron 2001). However, an important contrast is offered by our nearest giant neighbor, Andromeda (M31; NGC224). Although little is known about the formation history of M31, its halo has a strikingly higher metallicity (Mould & Kristian 1986; Holland, Fahlman, & Richer 1996; Durrell, Harris, & Pritchett 2001), despite its similar Hubble type to the Galaxy.

Hierarchical models suggest that spheroids (bulges and halos) form in a repetitive process during the mergers of galaxies and protogalaxies, while disks form by slow accretion of gas between merging events (e.g., White & Frenk 1991). The discovery of the Sgr dwarf galaxy (Ibata et al. 1994) sparked renewed interest in halo formation through accretion of dwarf galaxies. Ambitious programs are now mapping the spatial distribution, kinematics, and chemical abundance in the halos of the Galaxy (e.g., Morrison

et al. 2000; Majewski et al. 2000) and M31 (e.g., Ferguson et al. 2002). In the meantime, the overproduction of dwarf galaxies in hierarchical models has led to suggestions that most of the dwarfs formed in the early Universe have dissolved into the halo (e.g., Bullock et al. 2000). Whether or not such accretion is the dominant source of halo stars, it is likely that dwarf galaxies do contribute, with their stars sometimes remaining in coherent orbital streams for many Gyr. Indeed, such substructure has been found in the M31 halo (Ferguson et al. 2002).

With the installation of the Advanced Camera for Surveys (ACS; Ford et al. 1998) on the Hubble Space Telescope (HST), it is now possible to resolve the old main sequence population in the M31 halo and analyze the age distribution via the same techniques that have been applied to Galactic globular clusters (GCs) and satellite dwarf galaxies. M31 offers a unique testing ground for understanding giant galaxy formation, due to its proximity (770 kpc; Freedman & Madore 1990), small foreground reddening ( $E_{B-V} = 0.08$  mag; Schlegel, Finkbeiner, & Davis 1998), and low inclination ( $12.5^\circ$ ; de Vaucouleurs 1958). To investigate the star formation history of the M31 halo, we have obtained deep ACS observations of a minor axis field  $\approx 51$  arcmin (11 kpc) from the nucleus. In this initial report, we briefly describe the observations and report that the halo contains a significant population of intermediate age (6–8 Gyr) metal-rich ( $[\text{Fe}/\text{H}] > -0.5$ ) stars.

### 2. OBSERVATIONS AND DATA REDUCTION

Using the ACS Wide Field Camera, we obtained deep optical images of a field along the SE minor axis of the M31 halo, at  $\alpha_{2000} = 00^h46^m07^s$ ,  $\delta_{2000} = 40^\circ42'34''$ . The field is not as-

<sup>1</sup>Based on observations made with the NASA/ESA Hubble Space Telescope, obtained at the Space Telescope Science Institute, which is operated by AURA, Inc., under NASA contract NAS 5-26555. These observations are associated with proposal 9453.

sociated with the tidal streams and substructure found by Ferguson et al. (2002), and lies just outside the “flattened inner halo” in their maps. The field was previously imaged by Holland et al. (1996), using the Wide Field Planetary Camera 2 (WFPC2). Given the highly inclined disk, the contribution of disk stars at this position should be  $\lesssim 3\%$  (Walterbos & Kennicutt 1988; Holland et al. 1996 and references therein). We chose this field to optimize the crowding (trading off population statistics versus photometric accuracy) and to place an interesting M31 GC (GC312; Sargent et al. 1977) near the edge of our images; GC312 will be analyzed in a future paper.

From 2 Dec 2002 to 11 Jan 2003, we obtained 39.1 hours of images in the F606W filter (broad  $V$ ) and 45.4 hours in the F814W filter ( $I$ ), with every exposure dithered to allow for hot pixel removal, optimal point spread function sampling, smoothing of spatial variation in detector response, and filling in the gap between the two halves of the  $4096 \times 4096$  pix detector. We also obtained parallel WFPC2 observations of a field further out in the M31 halo, using the same filters; the WFPC2 data are much less deep than the ACS data, but they reach the MSTO, and will be analyzed in a forthcoming paper.

We co-added the M31 images using the IRAF DRIZZLE package, with masks for the cosmic rays and hot pixels, resulting in geometrically-correct images with a plate scale of  $0.03''$  pixel $^{-1}$  and an area of approximately  $210'' \times 220''$ . We then performed both aperture and PSF-fitting photometry using the DAOPHOT-II package (Stetson 1987), assuming a variable PSF constructed from the most isolated stars. The aperture photometry on isolated stars was corrected to true apparent magnitudes using TinyTim models of the HST PSF (Krist 1995) and observations of the standard star EGGR 102 (a  $V = 12.8$  mag DA white dwarf) in the same filters, with agreement at the 1% level. The PSF-fitting photometry was then compared to the corrected aperture photometry, in order to derive the offset between the PSF-fitting photometry and true apparent magnitudes. Our photometry is in the STMAG system:  $m = -2.5 \times \log_{10} f_{\lambda} - 21.1$ . For readers more familiar with the Johnson  $V$  and Cousins  $I$  bandpasses, a 5,000 K stellar spectrum has  $V - m_{F606W} = -0.05$  mag and  $I - m_{F814W} = -1.28$  mag.

Of the  $\sim 300,000$  stars detected, we discarded those within the GC312 tidal radius ( $10''$ ; Holland et al. 1997), within  $14.5''$  of a bright foreground star, within  $12.6''$  of this star’s window reflection, and near the image edges, leaving  $\approx 223,000$  stars in the final catalog. Using the SExtractor code (Bertin & Arnouts 1996), we estimate  $\lesssim 5\%$  of the stars are contaminated by extended sources. We show the CMD in Figure 1a. Extensive artificial star tests determine the photometric scatter and completeness as a function of color and luminosity. The CMD shows no obvious differences when comparing the population in a 10–100'' annulus around GC312 to that beyond 100''; the cluster does not appear to be associated with an extended underlying system. By integrating our catalog, we estimate that the surface brightness in our field is  $\mu_V \approx 26.3$  mag arcsec $^{-2}$ .

Our program includes ACS observations of four Galactic GCs spanning a wide metallicity range (Table 1), using the same filters, in order to obtain fiducials in these bands and to verify the transformation of theoretical isochrones to the observational plane. M92, NGC6752, and 47 Tuc are the most useful calibrators in our program, because their parameters are known very well; NGC6528 is also useful because of its high metallicity, but its parameters are less secure, and it suffers from high, spatially variable reddening (Heitsch & Richtler 1999). The GC images were not dithered, so these data were drizzled with-

out plate scale changes, in order to remove cosmic rays and to correct for geometric distortion. These images are significantly less crowded than those of M31, and the PSF is undersampled, so we performed aperture photometry but no PSF fitting, and corrected the aperture photometry to true apparent magnitudes.

TABLE 1: M31 and globular cluster parameters

Name	$(m - M)_V$ (mag)	$E_{B-V}$ (mag)	[Fe/H]
M31	24.68 <sup>a</sup>	0.08 <sup>b</sup>	-0.6 <sup>c</sup>
M92	14.60 <sup>d</sup>	0.023 <sup>b</sup>	-2.14 <sup>d</sup>
NGC6752	13.17 <sup>e</sup>	0.055 <sup>b</sup>	-1.54 <sup>f</sup>
47 Tuc	13.27 <sup>g</sup>	0.032 <sup>b</sup>	-0.83 <sup>f</sup>
NGC6528	16.15 <sup>h</sup>	0.55 <sup>h</sup>	-0.2 <sup>h</sup>

<sup>a</sup>Freedman & Madore (1990).

<sup>b</sup>Schlegel et al. (1998).

<sup>c</sup>Mould & Kristian (1986).

<sup>d</sup>VandenBerg & Clem (2003).

<sup>e</sup>Renzini et al. (1996).

<sup>f</sup>VandenBerg (2000).

<sup>g</sup>Zoccali et al. (2001).

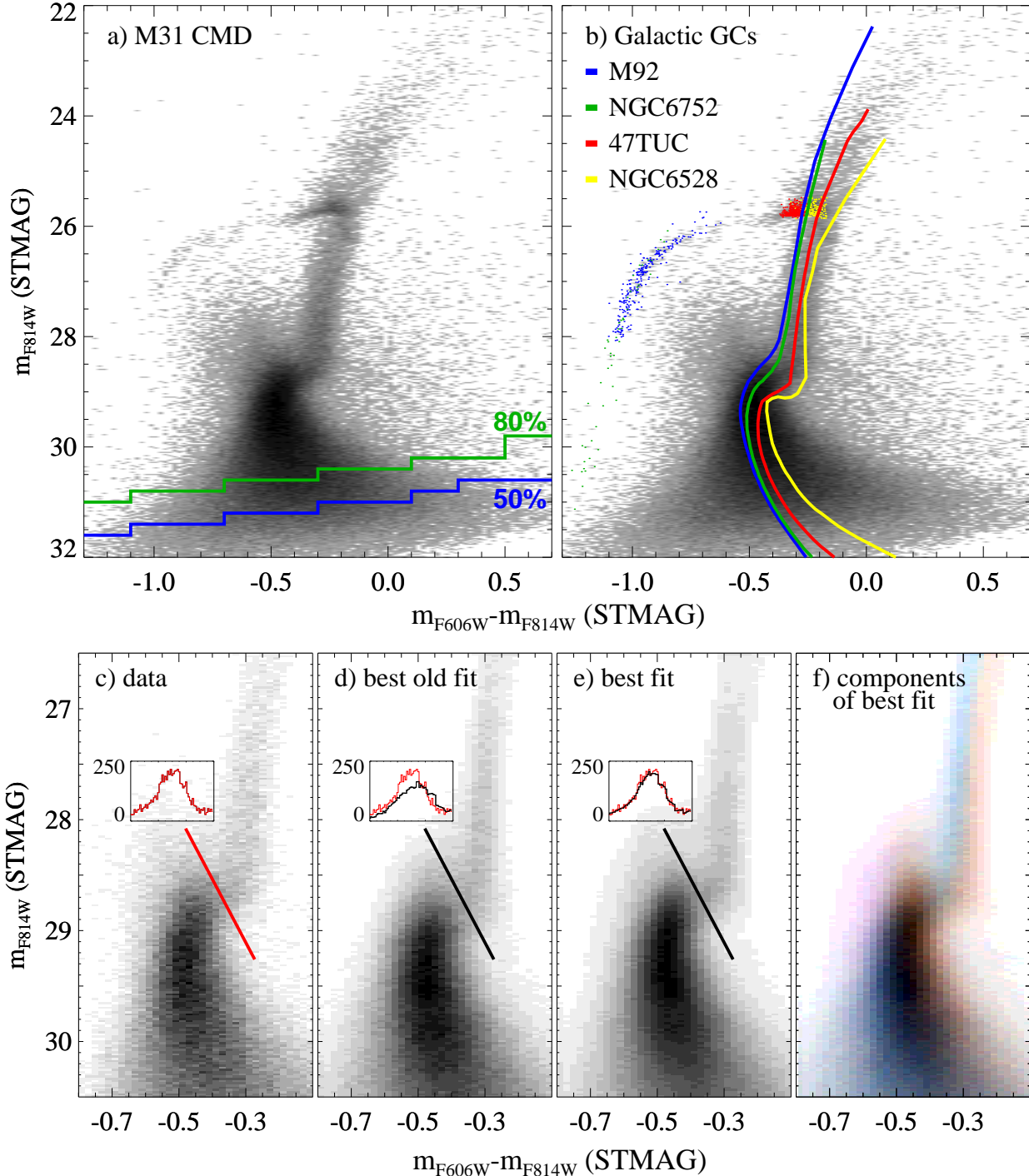
<sup>h</sup>Momany et al. (2003).

### 3. ANALYSIS

Our CMD reveals, for the first time, the main sequence population in the M31 halo. The horizontal branch (HB) extends from a well-populated red clump to a minority blue population ( $\sim 10\%$ ). The red giant branch (RGB) shows the broad color distribution extending to high metallicity, long-known to be characteristic of the M31 halo (Mould & Kristian 1986). The luminosity difference between the red HB and the RGB “bump” reaches 0.5 mag – another indication of near-solar metallicities. There is also a prominent blue plume of stars significantly brighter than the MSTO; this minority population ( $\sim 2\%$  the size of the population at the MSTO  $\pm 1$  mag) may include binaries, blue stragglers, or a residual young stellar population. Although the blue HB stars are characteristic of very old, metal-poor GCs (such as M92), the luminosity difference between the MSTO and HB is smaller than expected for a purely old stellar population. This is shown in Figure 1b, which includes the ridge lines and HB loci for the four GCs we observed with ACS. Also, the M31 subgiant branch is nearly horizontal, indicating a high metallicity, while its ridge is appreciably brighter than that of 47 Tuc and NGC6528, implying the presence of a significantly younger population in the M31 halo.

Our full analysis of the star formation history will be presented in a future paper. Here, we will supplement the comparisons shown in Figure 1b with examples from our modeling to date. Our modeling is based upon the isochrones of VandenBerg et al. (2003), which show good agreement with cluster CMDs spanning a wide range of metallicity and age. To transform these isochrones from the ground-based to HST-based bandpasses, we used the spectra of Lejeune, Cuisinier, & Buser (1997) to calculate  $V - m_{F606W}$  and  $I - m_{F814W}$ , then applied those differences to the ground-based magnitudes of the isochrones, with a small ( $\lesssim 0.05$  mag) empirical color correction to force agreement with our GC CMDs. After this correction, the isochrones match the ridge lines within  $\lesssim 0.02$  mag over the region of the CMD we are fitting. Our observed CMDs of these clusters are reproduced by a 12.5 Gyr isochrone for 47 Tuc and 14 Gyr isochrones for NGC6752 and M92. The isochrones do not include core He diffusion, which would reduce their ages by 10–12%,

FIG. 1– (a) The CMD of M31’s halo, shown as a Hess diagram with a logarithmic stretch and completeness limits (green and blue lines) labeled. (b) The M31 CMD with the ridge lines (colored curves) and HB stars (colored points) of 4 GCs overplotted. Except for NGC6528, the GCs have only been shifted by the differences in distance and reddening (Table 1). The NGC6528 ridge line and HB were shifted 0.16 mag brighter to align its HB to that of M31 (NGC6528’s distance and reddening are very uncertain). Note that much of the M31 subgiant branch is brighter than those of the clusters, indicating that M31’s halo is predominantly younger than Galactic GCs. (c) The region of the M31 CMD used for fitting the population age and metallicity distributions. The histogram (inset, red) shows the number of stars along a cut (red line) through the subgiant branch. (d) The best fit achieved using old (11–13.5 Gyr) isochrones spanning a range in metallicity ( $-2.31 < [\text{Fe}/\text{H}] < 0$ ). The inset compares the histogram (black) across the subgiant branch (black line) to that from the previous panel (red). Although the RGB width requires a spread in metallicity, old stars by themselves cannot reproduce the M31 CMD below the RGB. (e) The CMD for the best-fit population, with a significant spread in both age and metallicity. The two dominant components to the fit are a majority population of intermediate-age (6–11 Gyr) metal-rich ( $[\text{Fe}/\text{H}] > -0.5$ ) stars, and a smaller population of old (10–13.5 Gyr) metal-poor ( $[\text{Fe}/\text{H}] < -0.5$ ) stars. The inset compares a cut across the subgiant branch in the model (black) to that in the data (red), showing good agreement. (f) The same best-fit model, color-coded to highlight the intermediate-age metal-rich (red) and old metal-poor (blue) components.



thus avoiding discrepancies with the age of the Universe (VandenBerg et al. 2002).

Using isochrones with a range of ages and metallicities, we fit the region of the M31 CMD shown in Figure 1c using the StarFish code of Harris & Zaritsky (2001). Restricting the fit to this region of the CMD focuses on the most sensitive age and metallicity indicators while avoiding regions of the CMD that are poorly constrained by the models (e.g., the HB morphology). The StarFish code fits the observed CMD through a linear combination of input isochrones, using  $\chi^2$  minimization, where the isochrones are scattered according to the results of the artificial star tests. We first followed the standard method for determining the metallicity distribution from the RGB with a fit (not shown) to the RGB using a set of old (13.5 Gyr) isochrones spanning a wide metallicity range ( $-2.31 < [\text{Fe}/\text{H}] < 0$ ). The resulting metallicity distribution was similar to that found by Holland et al. (1996) in our same field, and Durrell et al. (2001) in a field 20 kpc from the nucleus. However, it was very obvious that the isochrones did not match the subgiant branch or the MSTO. Next, as shown in Figure 1d, we tried fitting the entire region of Figure 1c with a wider age range (11.5–13.5 Gyr), but found no acceptable combination. The insets of Figure 1c, d, and e are histograms showing the number of stars (data: *red*; model: *black*) along a cut through the subgiant branch (*thick line*). In Figure 1d, the residual subgiant stars that are not reproduced by this old model (*inset*) suggest that at least 20% of the stars in the halo must be younger than 11 Gyr. We conclude that a purely old stellar population cannot explain the CMD of the M31 halo.

Next, we expanded the age range to 6–13.5 Gyr and repeated the fit (see Figure 1e). The width of the RGB is now matched without a mismatch at the subgiant branch (*inset*). In Figure 1f, we highlight the two dominant populations in the best-fit model: 56% of the population (*red*) is metal-rich ( $[\text{Fe}/\text{H}] > -0.5$ ) and of intermediate age (6–11 Gyr), while 30% of the population (*blue*) is metal-poor ( $[\text{Fe}/\text{H}] < -0.5$ ) and old (11–13.5 Gyr). About half of this metal-rich population (i.e., 28% of the total population) is 6–8 Gyr old. We stress that these models only illustrate, in a broad sense, the dominant populations present in the M31 halo. Other combinations of young metal-rich and old metal-poor stars are possible. For example, we produced a similar fit by combining two very distinct isochrone groups: one at 6–8 Gyr with  $[\text{Fe}/\text{H}] > -1$ , and one at 11.5–13.5 Gyr with  $[\text{Fe}/\text{H}] < -1$ . In a future paper, we will

present more detailed constraints on the star formation history.

#### 4. SUMMARY AND DISCUSSION

The CMD of the M31 halo is evidently inconsistent with a population composed solely of old (GC-age) stars; instead, it is dominated by a population of metal-rich intermediate-age stars. Although the high metallicity in the M31 halo is well-documented, the large age spread required to simultaneously reproduce the RGB, subgiant, and main sequence distributions came to us as a surprise. Earlier studies of the RGB were insensitive to this age spread. For example, Durrell et al. (2001) were able to explain the metallicity distribution 20 kpc from the nucleus, with a simple chemical evolution model forming most of the stars at very early times (see also Côté et al. 2000). Although our field is relatively small in sky coverage, it appears representative; the metallicity in our field (Holland et al. 1996) agrees well with that much further out (Durrell et al. 2001), and there are no indications of substructure or tidal streams in the region we surveyed (Ferguson et al. 2002).

It seems unlikely that star formation in the halo proceeded for  $\sim 6$  Gyr from gas in situ; instead, the broad age dispersion in the halo is likely due to contamination from the disruption of satellites or of disk material into the halo during mergers. Indeed, our current analysis of the data cannot rule out the possibility that M31 and a nearly-equal-mass companion galaxy experienced a violent merger when the Universe was half its present age. If the 6–8 Gyr population in the halo represents the remnants of a disrupted satellite, the relatively high metallicity suggests that it must have been fairly massive. On the other hand, the stars could represent disruption of the M31 disk, either by a major collision when M31 was  $\sim 6$  Gyr old, or by repeated encounters with smaller satellites. The resulting halo would be a mix of the old metal-poor stars formed earliest in M31's halo, disk stars that formed prior to the merger(s), stars formed during the merger(s), and the remnant populations of the disrupted satellite(s).

Support for proposal 9453 was provided by NASA through a grant from STScI, which is operated by AURA, Inc., under NASA contract NAS 5-26555. We are grateful to J. Harris and P. Stetson for providing their codes and assistance. We thank the members of the scheduling and operations teams at STScI (especially P. Royle, D. Taylor, and D. Soderblom) for their efforts in executing a large program during a busy HST cycle.

#### REFERENCES

- Bertin, E., & Arnouts, S. 1996, *A&AS*, 117, 393  
 Bullock, J.S., Kravtsov, A.V., & Weinberg, D.H. 2000, *ApJ*, 539, 517  
 Côté, P., Marzke, R.O., West, M.J., & Minniti, D. 2000, *ApJ*, 533, 869  
 de Vaucouleurs, G. 1958, *ApJ*, 128, 465  
 Durrell, P.R., Harris, W.E., & Pritchett, C.J. 2001, *AJ*, 121, 2557  
 Ferguson, A.M.N., Irwin, M.J., Ibata, R.A., Lewis, G.F., & Tanvir, N.R. 2002, *AJ*, 124, 1452  
 Fontaine, G., Brassard, P., & Bergeron, P. 2001, *PASP*, 113, 409  
 Ford, H.C., et al. 1998, *Proc. SPIE*, 3356, 234  
 Freedman, W.L., & Madore, B.F. 1990, *ApJ*, 365, 186  
 Harris, J., & Zaritsky, D. 2001, *ApJS*, 136, 25  
 Heitsch, E., & Richtler, T. 1999, *A&A*, 347, 455  
 Holland, S., Fahlman, G.G., & Richer, H.B. 1996, *AJ*, 112, 1035  
 Holland, S., Fahlman, G.G., & Richer, H.B. 1997, *AJ*, 114, 1488  
 Ibata, R.A., Gilmore, G., & Irwin, M.J. 1994, *Nature*, 370, 194  
 Krist, J. 1995, ASP Conference Series 77, *Astronomical Data Analysis Software and Systems IV*, ed. R.A. Shaw, H.E. Payne, & J.J.E. Hayes, 349  
 Lejeune, T., Cuisinier, F., & Buser, R. 1997, *A&AS*, 125, 229  
 Majewski, S.R., Ostheimer, J.C., Kunkel, W.E., & Patterson, R.J. 2000, *AJ*, 120, 2550  
 Momany, Y., et al. 2003, *A&A*, 402, 607  
 Morrison, H.L., Mateo, M., Olszewski, E.W., Harding, P., Dohm-Palmer, R.C., Freeman, K.C., Norris, J.E., & Morita, M. 2000, *AJ*, 119, 2254  
 Mould, J., & Kristian, J. 1986, *ApJ*, 305, 591  
 Renzini, A., et al. 1996, *ApJ*, 465, L23  
 Ryan, S.G., & Norris, J.E. 1991, *AJ*, 101, 1865  
 Sargent, W.L.W., Kowal, C.T., Hartwick, F.D.A., van den Bergh, S. 1977, *AJ*, 82, 947  
 Schlegel, D.J., Finkbeiner, D.P., & Davis, M. 1998, *ApJ*, 500, 525  
 Sourbiran, C., Bienaymé, O., & Siebert, A. 2003, *A&A*, 398, 141  
 Stetson, P. 1987, *PASP*, 99, 191  
 VandenBerg, D.A., 2000, *ApJS*, 129, 315  
 VandenBerg, D.A., Bergbusch, P.A., & Dowler, P.D. 2003, in prep.  
 VandenBerg, D.A., & Clem, J.L. 2003, *AJ*, in press.  
 VandenBerg, D.A., Richard, O., Michaud, G., & Richer, J. 2002, *ApJ*, 571, 487  
 White, S.D.M., & Frenk, C.S. 1991, *ApJ*, 379, 52  
 Waltherbos, R.A.M., & Kennicutt, R.C., Jr. 1988, *A&A*, 198, 61  
 Zoccali, M., et al. 2001, *ApJ*, 553, 733